



Contents lists available at ScienceDirect

Journal of King Saud University – Science

journal homepage: www.sciencedirect.com



Original article

Tin oxide-chitosan-polyethylene glycol-D-pinitol nanocomposite ameliorates cardiac ischemia in diabetic rats *via* activating p62/Keap1/Nrf2 signaling

Hou Rongrong^{a,1}, Yin Tao^{b,1}, Kong Ying^a, Jia Fang^a, Jiang Wei^c, Yang Qiang^c, Xu Jing^{a,*}^a Department of Endocrinology, the Second Affiliated Hospital, Xi'an Jiaotong University, Xi'an 710032, China^b Department of Cardiology, the First Affiliated Hospital, Air Force Medical University, Xi'an 710032, China^c Department of Cardiology, the Second Affiliated Hospital, Xi'an Jiaotong University, Xi'an 710032, China

ARTICLE INFO

Article history:

Received 18 June 2021

Revised 30 December 2021

Accepted 6 January 2022

Available online 13 January 2022

Keywords:

Diabetes

Myocardial ischemia

Streptozotocin

D-Pinitol

SCP-D-P nanocomposites

p62/Keap1/Nrf2 pathway

ABSTRACT

Diabetes is a silent killer with increased global public health burden along with several life threatening complications. Myocardial infarction was diagnosed in 60% of diabetic patients worldwide. In this study, the synthesized nanocomposites were subjected to Ultraviolet-Visible Spectroscopic analysis, Photoluminescence Spectroscopic analysis, X-ray diffraction (XRD), Fourier-transform infrared spectroscopy (FTIR), dynamic light scattering (DLS) and Field Emission Scanning Electron Microscope (FE-SEM) & energy dispersive X-ray analysis (EDAX) analysis. Further in vivo studies were performed on young male Wistar rats. Young male Wistar rats were induced diabetes with streptozotocin induced diabetes model and the diabetic rats confirmed with blood glucose were utilized for further study. The rats were grouped into control, diabetic, diabetic induced treated with 5 mg/kg of SCP-D-P nanocomposites and diabetic induced treated with 10 mg/kg of SCP-D-P nanocomposites. After treatment period the rats were estimated for diabetic functioning parameters such as glucose level, insulin level, c-peptide, HOMA-IR and cardiac functioning parameters such as total cholesterol, triglycerides, CK, LDH, MDA, NO, GSH, CAT, SOD, GST. Rats were subjected to echocardiography analysis for assessing the cardiac function. Inflammatory markers TNF- α and IL- β were estimated to analyze the anti-inflammatory property of SCP-D-P nanocomposites and it is further confirmed with histopathological analysis of cardiac tissue with H&E staining. Further we assessed the impact of SCP-D-P nanocomposites on p62/Keap1/Nrf2 signaling pathway which is plays a vital role in myocardial ischemia. Our results of nanocomposite analysis depicts SCP-D-P nanocomposites is a potent nanoparticles which persuasively decreased the diabetic inducing factors, ameliorated cardiac functioning. Histological analysis clearly depicts SCP-D-P nanocomposites prevented diabetic induced cardiac tissue damage via activating p62/Keap1/Nrf2 signaling pathway. Over all our results confirms SCP-D-P nanocomposites is potent anti-diabetic, cardioprotective molecule.

© 2022 The Authors. Published by Elsevier B.V. on behalf of King Saud University. This is an open access article under the CC BY-NC-ND license (<http://creativecommons.org/licenses/by-nc-nd/4.0/>).

1. Introduction

Diabetes a silent killer is a global burden both to the health sector and the financial sector. The incidence rate of diabetes is drastically increases in the age group of people between 20 and 79 years

(Bommer et al., 2017). By the year 2045 the number of diabetic patients globally will increase to 693 millions. World Health Organization (WHO) had declared diabetes has serious pathology of the 21st century and it ranks seventh leading cause of death in the year 2016 (GBD, 2015; WHO, 2016; Cho et al., 2018). The prolonged diabetic condition in patients leads to various other complication which is classified as macro and microvascular complications. Macrovascular complication includes stroke, coronary artery disease and peripheral arterial disease whereas microvascular complications include retinopathy, neuropathy, nephropathy etc (Harding et al., 2019). Myocardial infarction was diagnosed in 60% of diabetic patients and the risk of developing myocardial infarction is 6–10 times higher in diabetic patients compared to non-diabetic patients (Ferannini et al., 2020; Dedov et al., 2015). American Heart Associa-

* Corresponding author.

E-mail address: xujdoctor@sina.com (X. Jing).¹ Equal contribution.

Peer review under responsibility of King Saud University.



Production and hosting by Elsevier

<https://doi.org/10.1016/j.jksus.2022.101827>

1018-3647/© 2022 The Authors. Published by Elsevier B.V. on behalf of King Saud University.

This is an open access article under the CC BY-NC-ND license (<http://creativecommons.org/licenses/by-nc-nd/4.0/>).

tion (AHA) had published treating diabetic patients with cardiovascular disease is more complicated than the non-diabetic patients (Arnold et al., 2020).

Nanotechnology is an emerging field with wide applications in various areas such as engineering, food industries, clothing industries, cosmetics, medical diagnostics, pharmaceutical etc (Chadha 2013). The role of nanotechnology in the field of medicine is a promising hope for the health care workers and patients with various chronic diseases. Nanoparticles were used in drug delivery system, vaccinations, implantation of nanotransmitter helps to monitor patient at microlevel (Kaurav et al., 2018). The biocompatible nature and the size with increased surface, increased cell permeability and target specific properties of nanoparticles to be utilized in the medical field. Various types of nanoparticles are synthesized such as silver, zinc, gold etc. besides tin oxide nanoparticles possess numerous pharmacological properties such as antioxidant, cytotoxic, antibacterial etc (Roopan et al., 2015; Vidhu and Philip, 2015). Nanocomposites are lighter in weight and utilized as novel drug nanocarriers due to their surface properties (Ali and Ahmed, 2018). Thus synthesizing nanocomposite with tin oxide may be effective nanomedicine to treat diabetic associated myocardial ischemia.

Recently, phytomedicine plays a vital role in treating various chronic diseases in particular life style diseases such as diabetes, hypercholesterol, obesity etc. The bioactive compounds in medicinal herbs were classified based on their structure and functional properties. D-Pinitol, 3-O-methyl-D-chiro-inositol is cyclitol which is present mostly in the plants belonging to Leguminosae and Pinaceae. It is also present in fenugreek seeds, soybean, ice plant and species of Retama genus which is consumed as food and also used in traditional medicines (Lee et al., 2014; Lahuta et al., 2018; Christou et al., 2019). It possess various pharmacological properties such as anticancer (Rengarajan et al., 2012), antidiabetic (Gao et al., 2015), anti inflammatory (Zheng et al., 2017), antioxidant (Lee et al., 2019), antitumor (Lin et al., 2013) etc.

The cardioprotective property of D-pinitol was not yet elucidated hence in the present study we analyzed the cardioprotective effect of D-pinitol-based nanocomposites in diabetic rats those are highly risk group for cardiac complications and more complicated to be treated. D-pinitol, the phytochemical was incorporated in tin oxide-chitosan-polyethylene glycon polymer to increase its efficacy and its role in the activation of p62/Keap1/Nrf2 signaling pathway in the diabetic rats were studied.

2. Materials & methods

2.1. Preparation of tin oxide – chitosan – polyethylene glycol – D pinitol (SCP-D-P) nanocomposites

SCP-D-P nanocomposites were prepared in the laboratory with tin oxide nanoparticles. To 20 ml of chitosan solution, 0.3 g of tin oxide nanoparticles was added and the chitosan-tin oxide nanoparticles mixture was further added to 20 ml of polyethylene glycol to form a Tin oxide-Chitosan-PEG nanocomposite. Tin oxide-Chitosan-PEG nanocomposite was further encapsulated with 50 μ l of D-pinitol solution by placing on a hot plate at 80 °C for 6 h with continuous stirring. After 6 h incubation white precipitate was formed and the solution was subjected to centrifugation at 15,000 rpm for 15 min at –4. The sediment was collected and washed thrice with deionized water and dried at 200 °C for 3 h. The powdered nanoparticles were stored in sterile vials and subjected to further characteristic analysis.

2.2. Ultraviolet-visible spectroscopic analysis

SCP-D-P nanocomposites were subjected to UV-Vis spectroscopic analysis with Perkin Elmer, (USA). The samples were placed

in quartz cuvette and analyzed between the wavelength 1200 and 200 nm. The experiments were performed thrice and the data were analyzed.

2.3. Photoluminescence Spectroscopic analysis

SCP-D-P nanocomposites photoluminescence spectroscopic analysis was done on the based on the spectra results obtained at λ_{exc} = 405 nm (Roithner Laser Technik, Germany). The experiment was performed thrice and the results were subjected to further analysis.

2.4. X ray diffraction (XRD) analysis

XRD pattern of SCP-D-P nanocomposites was assessed in D8 Advance Bruker system. The system is equipped with copper scintillation counter and the samples were subjected to analysis at 45 mA and 40 kV voltage. The samples were scanned for about 0.02–0.5 sec and the results were noted.

2.5. Fourier transform infra red (FT-IR) spectroscopic analysis

The SCP-D-P nanocomposites were subjected to infra red analysis in Nicolet iS50. The sample was mixed with potassium bromide pellets and the mixture was placed on to the scanning disc. The samples were scanned between the wavelengths of 500 and 4000 cm^{-1} .

2.6. Dynamic light scattering (DLS) analysis

The hydrodynamic radii of SCP-D-P nanocomposites were determined with DLS studies using Nano-ZS (Malvern).

2.7. Field emission-scanning electron microscope (FE-SEM) & energy dispersive X-ray (EDAX) analysis

The synthesized SCP-D-P nanocomposites were subjected to field- emission scanning electron microscope FE-SEM, s-4800II, Hitachi, 15 kV equipped with EDAX.

2.8. Experimental animals

Young male Wistar rats were used as experimental animals in the current study. All rats were utilized in this study were recognized with standard attention in compliance with protocols by the National Institutes of Health, United States. The rats were procured from Xi'an Jiaotong University, Xi'an, 710032, China and the procedure to be performed on rats was clearly explained before the ethical committee Xi'an Jiaotong University Health Science Center (IAEC No: 2019-1077). The rats were maintained in clean laboratory condition and the bedding was changed for every two days. The rats were fed with standard laboratory pellet diet ad libidum. The rats were treated with utmost care and concern and no mortality was observed throughout the experimental period.

2.9. Induction of diabetes

Streptozotocin (STZ) induced diabetes model was chosen for the current study to induce diabetes in rats. The rats were injected with single intraperitoneally dose of 35 mg/kg STZ dissolved in 0.1 M citrate buffer (pH 4.4) in high fat diet fed rats. The induction of diabetes was confirmed after 14 days of STZ shot by estimating the blood glucose levels. 11 mmol/l was considered as reference value the rats which had more than 11 mmol/L was considered diabetic and used in the present study

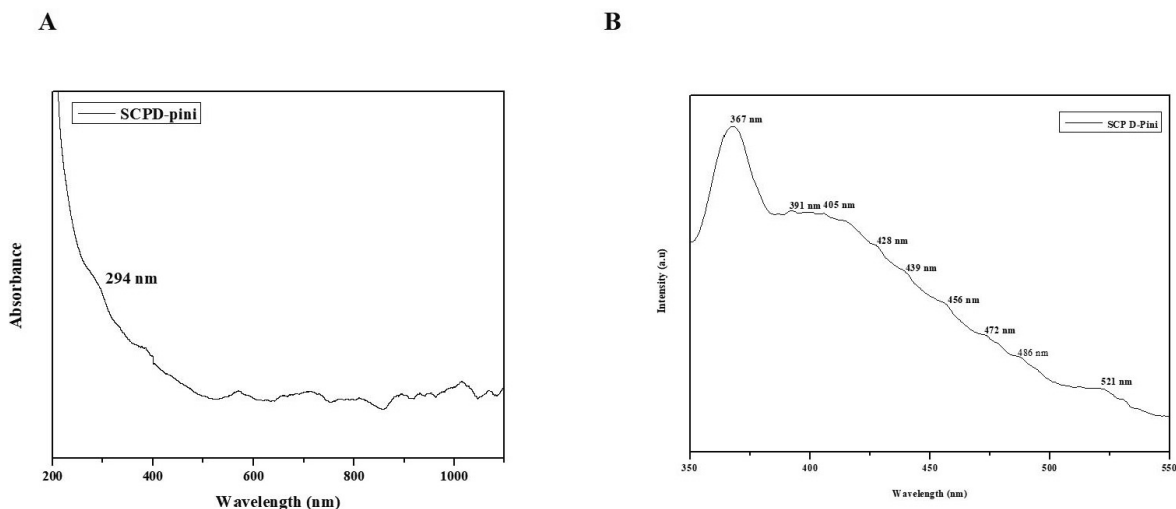


Fig. 1. Characterization of nanocomposites. Spectroscopic analysis. Ultraviolet–Visible Spectroscopic analysis (A) and photoluminescence Spectroscopic analysis (B) of synthesized SCP-D-P nanocomposites.

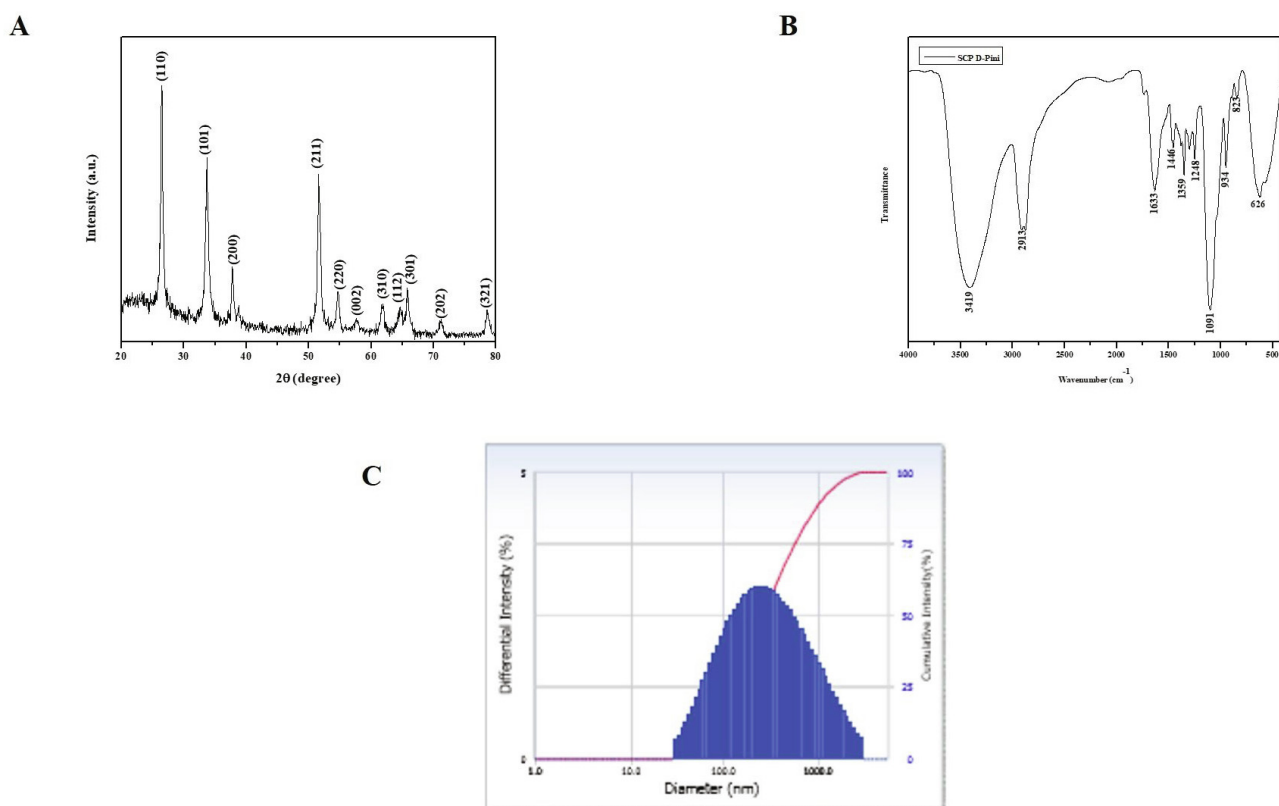


Fig. 2. Characterization of nanocomposites. X-ray Diffraction analysis (A), Fourier Transform Infra Red spectroscopic analysis (B), Dynamic Light Scattering Analysis (C) of synthesized SCP-D-P nanocomposites.

2.10. Experimental design

The rats were grouped into 4 Group I rats control rats – healthy non diabetic rats, Group II – Diabetic rats received only saline throughout the experimental period,

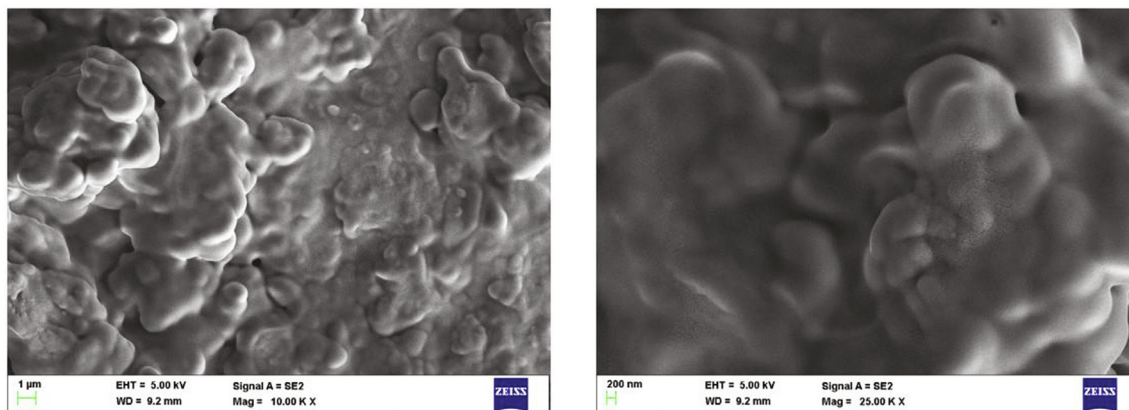
Group-III – Diabetic induced rats were treated with 5 mg/kg of SCP-D-P nanocomposites through oral gavage and Group IV – Dia-

betic induced rats were treated with 10 mg/kg of SCP-D-P nanocomposites.

2.11. Estimation of glucose

The fasting blood sugar of control, diabetic and diabetic treated with SCP-D-P nanocomposites. The fasting retro orbital blood was

A



B

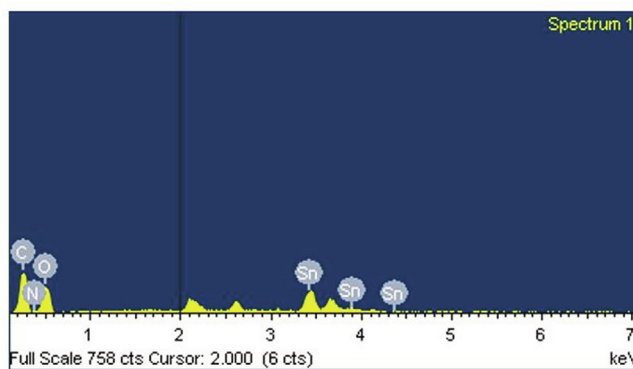


Fig. 3. Characterization of nanocomposites. Field emission scanning electron microscopic analysis & EDAX analysis of synthesized SCP-D-P nanocomposite.

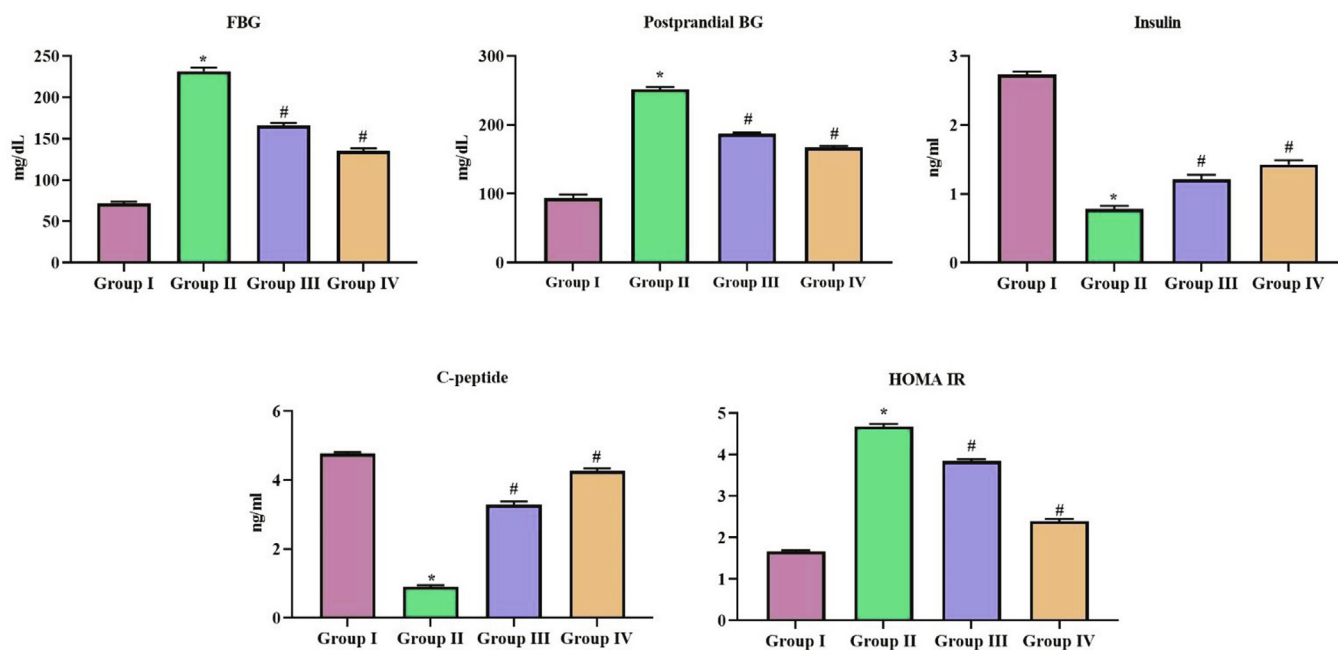


Fig. 4. Hypoglycemic effect of SCP-D-P nanocomposites in diabetic induced rats. T. The non diabetic control (Group I), diabetic induced (Group II), diabetic induced SCP-D-P nanocomposites low (Group III) and high dose (Group IV) treated rats were assessed for insulin resistance. FG- Fasting glucose, post prandial blood glucose levels, insulin, c-peptide and HOMA-IR value. Experiments were performed with commercially available kits. Each bar shows the mean \pm SD of triplicates and '# p < 0.05 was considered as statistically significant.

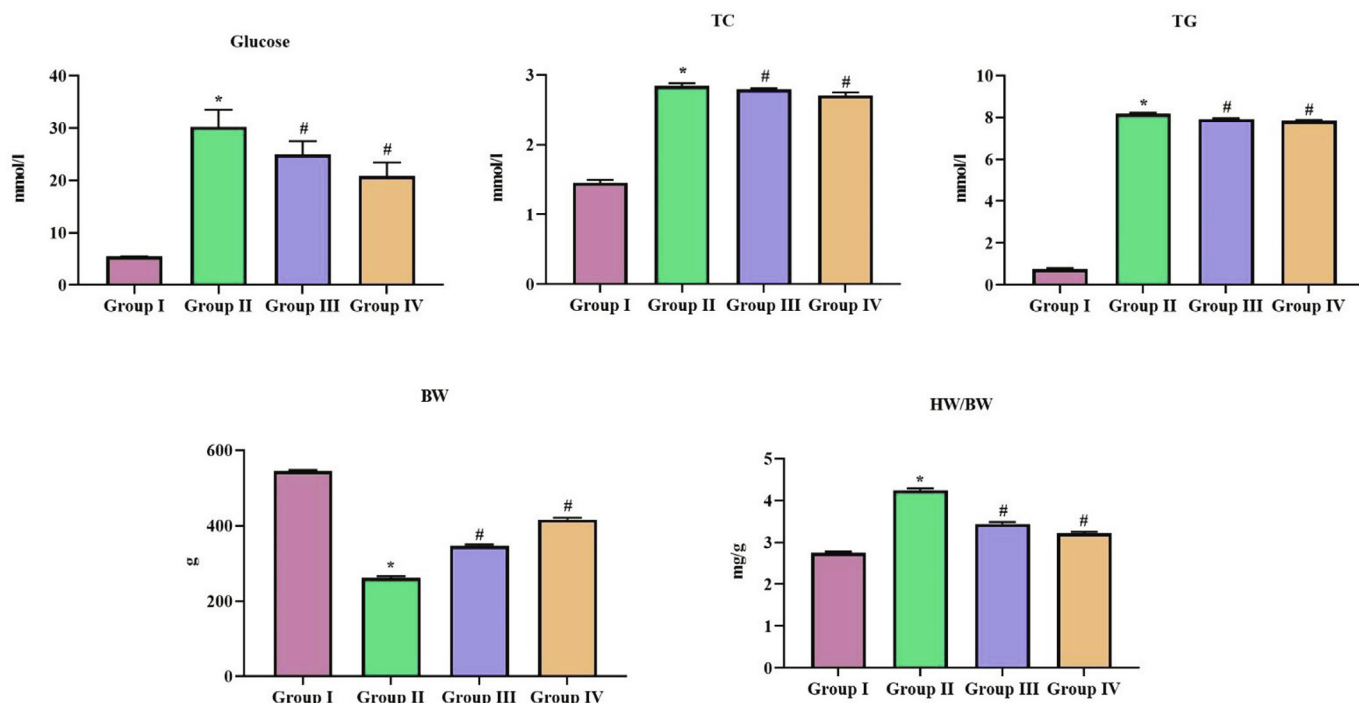


Fig. 5. Hypocholesterolemic effect of SCP-D-P nanocomposites in diabetic induced rats. The non diabetic control (Group I), diabetic induced (Group II), diabetic induced SCP-D-P nanocomposites low (Group III) and high dose (Group IV) treated rats were assessed for TC – Total cholesterol, TG – Triglycerides to assess the cholesterol levels. Experiments were performed with commercially available kits. BW – Bodyweight and HW – Heart weight were also measured. Each bar shows the mean ± SD of triplicates and '#' p < 0.05 was considered as statistically significant.

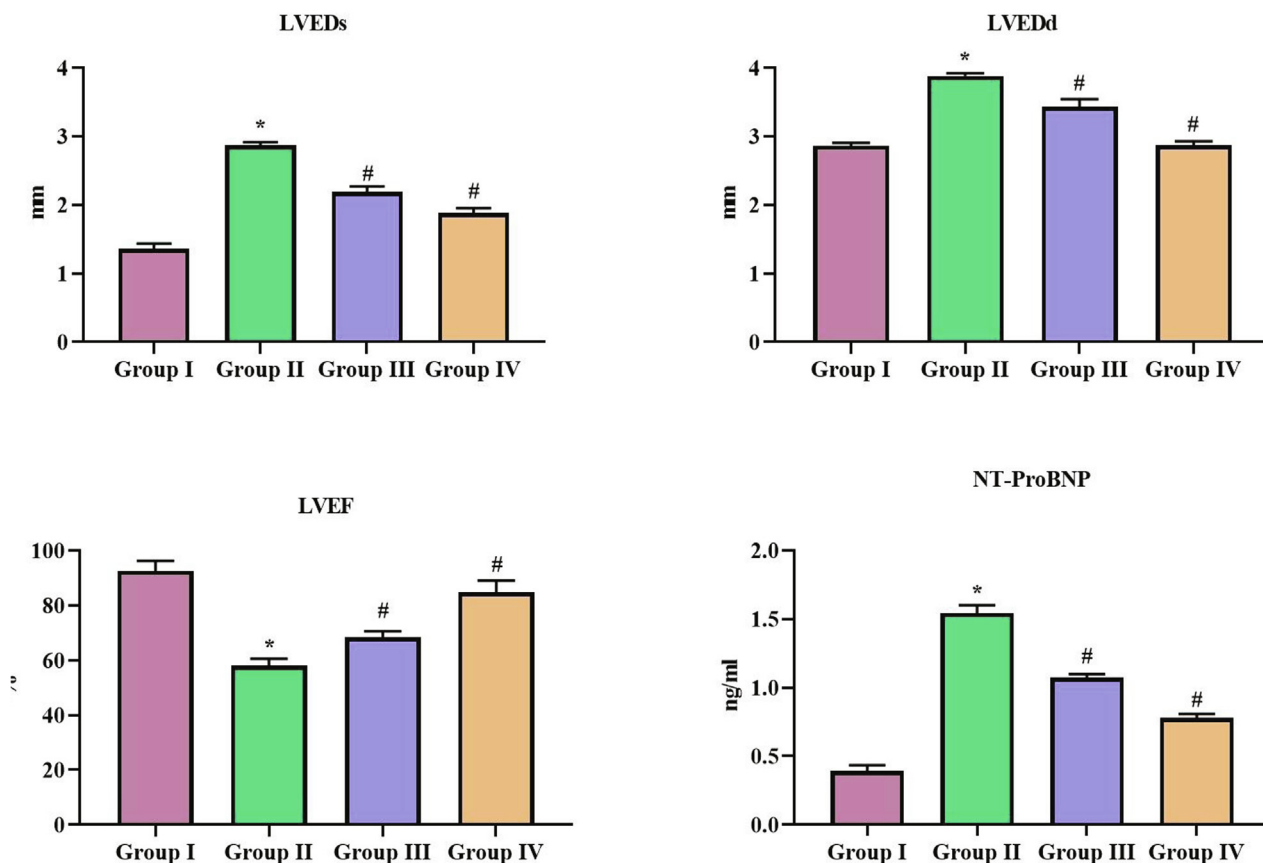


Fig. 6. Effect of SCP-D-P nanocomposites on cardiac function in diabetic induced rats. The non diabetic control (Group I), diabetic induced (Group II), diabetic induced SCP-D-P nanocomposites low (Group III) and high dose (Group IV) treated rats were assessed for cardiac function with echocardiographic analysis. LVEDs – Left ventricular end systolic diameter, LVEDd – Left ventricular end diastolic diameter, LVEF – Left ventricular ejection factor and NT-proBNP – N-terminal pronatriuretic peptide. Each bar shows the mean ± SD of triplicates and '#' p < 0.05 was considered as statistically significant.

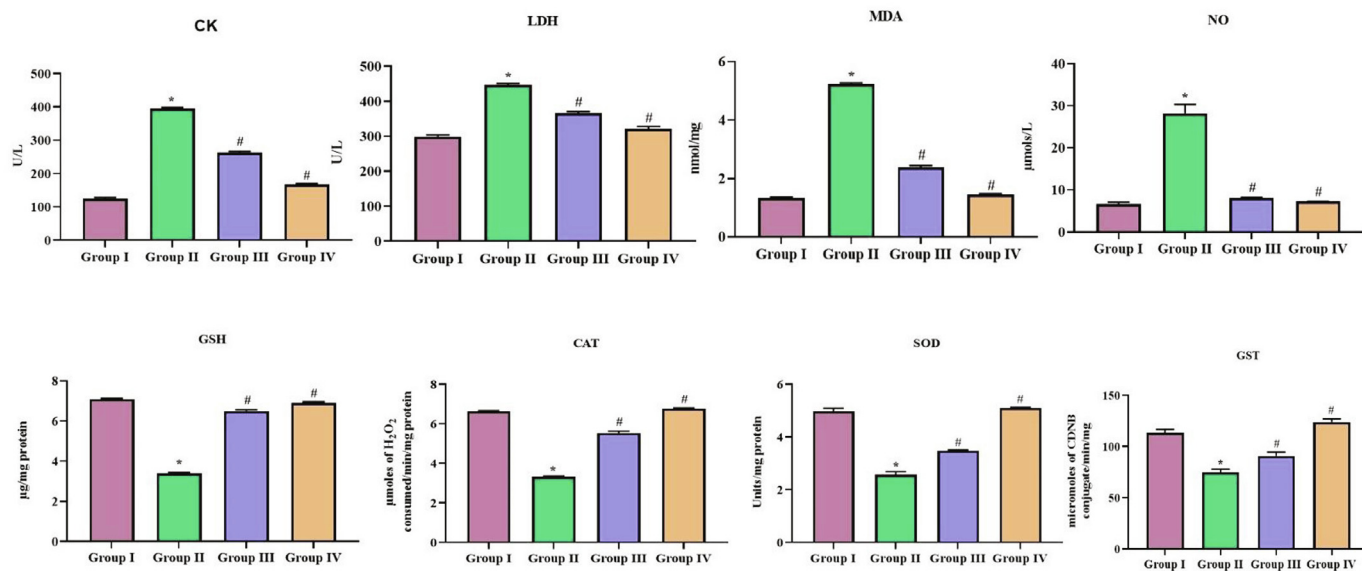


Fig. 7. Cardioprotective effect of SCP-D-P nanocomposites in diabetic induced rats. The non diabetic control (Group I), diabetic induced (Group II), diabetic induced SCP-D-P nanocomposites low (Group III) and high dose (Group IV) treated rats were assessed for CK – creatine kinase, LDH – lactate dehydrogenase, MDA – malondialdehyde, NO – nitric oxide, GSH – glutathione, CAT – catalase, SOD – superoxide dismutase and GST – glutathione-S-transferase to analyze cardiac functioning. Experiments were performed with commercially available kits. Each bar shows the mean ± SD of triplicates and ‘#’ p < 0.05 was considered as statistically significant.

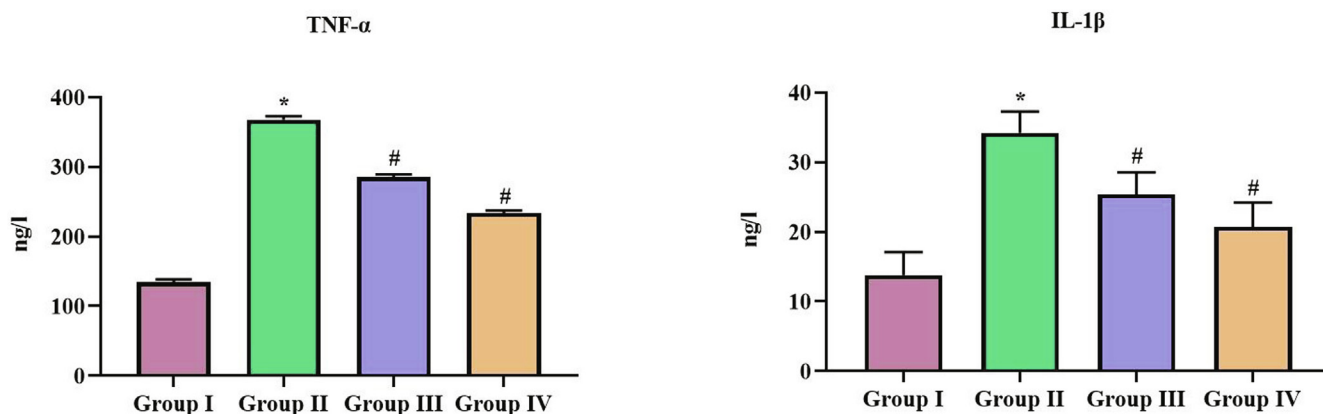


Fig. 8. Anti-inflammatory effect of SCP-D-P nanocomposites in diabetic induced rats. The non diabetic control (Group I), diabetic induced (Group II), diabetic induced SCP-D-P nanocomposites low (Group III) and high dose (Group IV) treated rats were assessed for pro inflammatory cytokines TNF-α, IL-1β to analyze the anti-inflammatory effect. Experiments were performed with commercially available kits. Each bar shows the mean ± SD of triplicates and ‘#’ p < 0.05 was considered as statistically significant.

collected early morning for the estimation of fasting blood sugar. The blood sugar levels were estimated with glucose estimation kit purchased from Crystal Chem, USA.

2.12. Estimation of insulin & C peptide

The postprandial levels of insulin were estimated in control, diabetic and diabetic treated with SCP-D-P nanocomposites. Insulin was estimated with ELISA kit purchased from BioCompare, USA and the c-peptide levels were estimated with ELISA kit purchased from RayBiotech. The procedures were followed as per the manufacturer’s protocol.

2.13. Homeostasis model assessment–insulin resistance (HOMA-IR) value

HOMA-IR value of control, diabetic and diabetic treated with SCP-D-P nanocomposites was calculated using the formula.

$$\text{HOMA-IR} = \text{Fasting glucose (mMol/l)} \times \text{Fasting insulin (}\mu\text{U/ml)} / 22.5.$$

2.14. Body weight

The body weight of the control and experimental rats were estimated and the means values were recorded. The relative heart

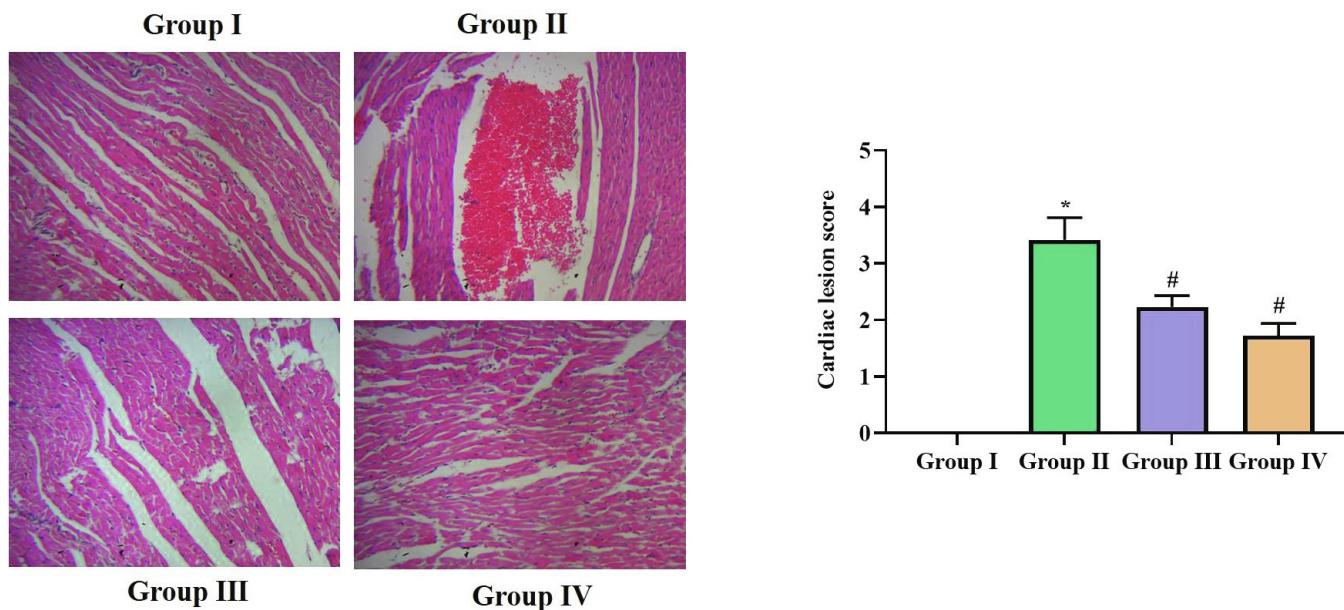


Fig. 9. Effect of SCP-D-P nanocomposites of cardiac tissues of diabetic induced rats. Longitudinal section of H&E stained cardiac tissues of non diabetic and SCP-D-P nanocomposites treated diabetic induced rats. (Group I) Control non diabetic rats (Group II) Diabetic induced rats (Group III) Diabetic induced 5 mg/kg SCP-D-P nanocomposites treated rats (Group IV) Diabetic induced 10 mg/kg SCP-D-P nanocomposites treated rats.

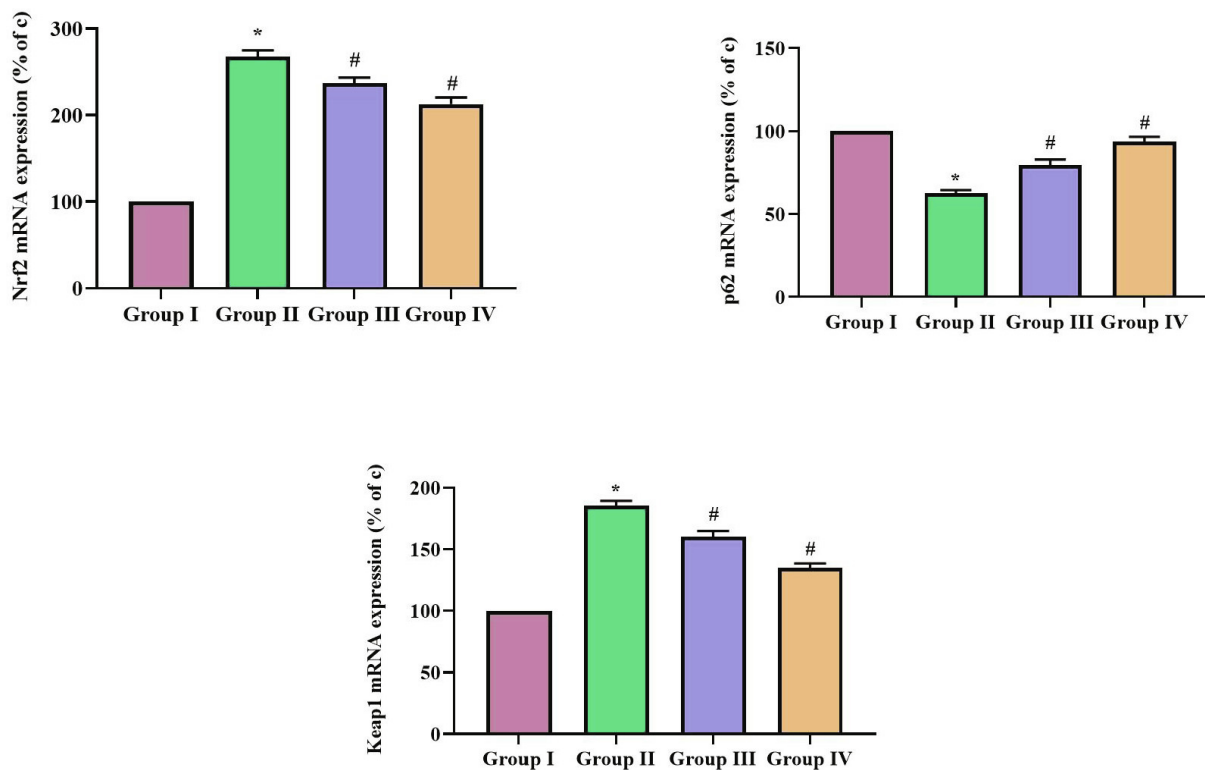


Fig. 10. Effect of SCP-D-P nanocomposites on p62/Keap1/Nrf2 signaling in diabetic induced rats. The non diabetic control (Group I), diabetic induced (Group II), diabetic induced SCP-D-P nanocomposites low (Group III) and high dose (Group IV) treated rats were assessed for p62, Keap1, Nrf2 gene expression using RT-PCR analysis. The percentage of increase gene expression was assessed with Quantity One Software and the values were depicted as graph. Each bar shows the mean \pm SD of triplicates and '#' $p < 0.05$ was considered as statistically significant.

weight of each rat was also measured to assess the impact of diabetes on heart.

2.15. Biochemical analysis

The total cholesterol and triglycerides were estimated in the serum of experimental rats. Total cholesterol and triglycerides were estimated with the kits purchased from Sigma Aldrich USA. The experiment was carried as per the manufacturer's protocol.

2.16. Echocardiography analysis

The rats were anesthetized with 1.5% isoflurane and placed on heating pad to maintain normothermia. The rats were subjected to transthoracic echocardiography analysis with high resolution micro imaging system (Visual Sonic Vevo 2100) with 40 MHz transducer. The heart rate and ECG of the rat were continuously monitored throughout the procedure. The hearts were imaged to assess left ventricular end systolic diameter, left ventricular end diastolic diameter, left ventricular ejection fraction and N-terminal proatriuretic peptide.

2.17. Cardiac marker analysis

The cardiac markers were estimated with the kits the commercially available creatine kinase was quantified with the kit procured from ThermoFischer Scientific, USA, lactate dehydrogenase, Glutathione S-transferase from MyBioSource, USA, lipid peroxidation assay, super oxide dismutase from BioVision, nitric oxide, glutathione and catalase activity were estimated from the kits procured from Sigma Aldrich, USA. The experiments were performed according to the manufacturer's protocol.

2.18. Estimation of proinflammatory cytokines

The estimation of cytokines tumor necrosis factor- α (TNF- α), interleukin (IL)-1 β was quantified with commercially available ELISA kit procured from Invitrogen, USA. The experiment was performed as per the manufacturer's protocol. The absorbance of samples was measured at 405 nm and the concentration of samples was calculated based on standard curve drawn.

2.19. Histopathological analysis

Haematoxylin & Eosin (H&E) staining was performed to analyze the ameliorating effect nanocomposite against histopathological damage caused due to diabetic induction. The formalin fixed cardiac tissue were subjected tissue processing and the tissues were fixed with paraffin wax blocks. The blocks were sectioned into 5microns sections using rotary microtome and the sections deparaffinized in a hot water bath. The section were then coated on to an albumin coated slides and stained with H&E stains. The sections were then visualized under light microscope and photographed. The images were then assessed for cardiac lesion score with ImageJ software.

2.20. RT-PCR analysis

The cardiac tissue of control, diabetic and diabetic induced SCP-D-P nanocomposites treated rats were subjected to RT-PCR analysis to quantify the m-RNA expression of p62, Nrf2 and Keap1 proteins which plays a vital role in myocardial ischemia. 1 mg of tissues were homogenized with 1 ml of TriZOL reagent and to the homogenate 500 μ l chloroform was added and centrifugation for 10,000 rpm 15 min at 4 °C. The supernatant was collected and to the equal amount isopropanol was added to precipitate RNA. The

mixture was subjected to centrifugation for 12,000 rpm 15 min at 4 °C and the pellet was collected after centrifugation. The RNA pellet was rinsed with 70% ethanol thrice and the pellet was air dried in clean chamber. The RNA was then dissolved with sterile milliQ water and subjected to RNA quantification with NanoDrop spectrophotometer. The RNA was converted to cDNA using the HiScript II Q RT SuperMix kit (Vazyme, China) and utilized for RT-PCR analysis. The PCR analysis was done with KAPATaq Ready Mix DNA Polymerase in thermocycler with specific thermocyclic condition. The amplified PCR products were then subjected to gel electrophoresis with 2% agarose gel. The gel were scanned to detect the band density of cDNA products and each gene were normalized with internal control gene β -actin. The band intensities were quantified with Quantity One Software (BioRad, USA).

2.21. Statistical analysis

The data obtained were statistically assessed with statistics software GraphPad Prism, USA. Analysis of Variance (ANOVA) was used to find the difference between groups and the Student's Newman-Keuls post hoc test was done. In all cases $p < 0.05$ was considered as statistically significant.

3. Results

3.1. Characterization of nanocomposites

3.1.1. Spectroscopic analysis

The spectroscopic analysis of synthesized nanocomposite was performed with Ultraviolet–Visible Spectroscopic analysis and photoluminescence Spectroscopic analysis and the results were depicted in Fig. 1A&B. UV–Vis spectroscopic analysis shows an absorbance band at 294 nm and photoluminescence Spectroscopic analysis shows a sharp band at 367 nm which confirms the synthesis of SCP-D-P nanocomposites.

3.1.2. XRD analysis

Fig. 2A depicts the results X-ray diffractometer pattern of SCP-D-P nanocomposites and peaks were observed in 110, 101, 200, 211, 220, 312, 112, 301, 321 indicating a crystalline structure of SCP-D-P nanocomposites.

3.1.3. FT-IR spectroscopic analysis

Fig. 2B illustrates the FT-IR results of SCP-D-P nanocomposites. Distinctive vibration patterns were observed between the wave length of 3500–600. The bands obtained at 823 and 626 may be due to the stretching vibration of tin oxide. The band obtained at 3419, 1613, 1248, 1091 are due to stretching vibration of O–H, C=O, C–OH, C=O respectively.

3.1.4. DLS analysis

Fig. 2C shows the results of dynamic light scattering analysis of SCP-D-P nanocomposites. The graph represents the average size of nanocomposite as 150 nm and it is also confirmed with XRD analysis.

3.1.5. FE-SEM & EDAX analysis

SCP-D-P nanocomposites were subjected to FE-SEM analysis to assess the surface morphology and the results were depicted in Fig. 3. The images shown spherical structure of nanocomposites agglomerated together. Further EDAX analysis was performed to confirm the presence of tin. Sharp characteristic peaks were found in EDAX graph which indicates presence of tin. Distinctive peaks were found lesser than 1 keV may be due to carbon, nitrogen and oxygen exhibited by pinitol.

3.1.6. Hypoglycemic effect of SCP-D-P nanocomposites in diabetic induced rats

Fig. 4 depicts the glycemic status of SCP-D-P nanocomposites treated diabetic induced rats. Compared to diabetic rats the levels of both fasting and post prandial blood sugar levels were decreased in SCP-D-P nanocomposites treated diabetic induced rats. Insulin and c-peptide levels were increased in SCP-D-P nanocomposites treated diabetic induced rats compared to diabetic untreated rats. C-peptide levels of 10 mg/kg SCP-D-P nanocomposites treated rats were comparatively equal to the levels of control non-diabetic rats. HOMA-IR value is decreased in SCP-D-P nanocomposites treated diabetic induced rats compared to diabetic untreated rats.

3.1.7. Hypocholesterolemic effect of SCP-D-P nanocomposites in diabetic induced rats

Fig. 5 shows the results of the total cholesterol and triglycerides levels in SCP-D-P nanocomposites treated diabetic induced rats. Compared to diabetic rats the total cholesterol levels were decreased in SCP-D-P nanocomposites treated diabetic induced rats. No significant difference observed between the levels in triglycerides of diabetic untreated and SCP-D-P nanocomposites treated diabetic induced rats.

3.1.8. Effect of SCP-D-P nanocomposites on body weight in diabetic induced rats

Diabetic induced untreated rats shown a drastic decrease in body weight compared to the control rats whereas SCP-D-P nanocomposites treated diabetic induced rats shown increase in the body weight compared to diabetic induced rats. The relative heart weight of SCP-D-P nanocomposites treated diabetic induced rats were decreased than the diabetic induced untreated rats.

3.1.9. Effect of SCP-D-P nanocomposites on cardiac function in diabetic induced rats

Cardiac functioning of SCP-D-P nanocomposites treated diabetic induced rats were assessed with echocardiographic analysis and the results were tabulated in Fig. 6. The left ventricular end systolic and diastolic diameter were decreased in SCP-D-P nanocomposites treated diabetic induced rats compared to the diabetic untreated rats. Left ventricular ejection factor is significantly decreased in diabetic induced untreated rats compared to the control rats. SCP-D-P nanocomposites treated diabetic induced rats shown significant increase in left ventricular ejection factor. N-terminal proatriuretic peptide levels were drastically increased in diabetic induced untreated rats compared to control non diabetic rats. SCP-D-P nanocomposites treated diabetic induced rats shown significant decrease in the N-terminal proatriuretic peptide levels compared to diabetic induced untreated rats.

3.2. Cardioprotective effect of SCP-D-P nanocomposites in diabetic induced rats

Fig. 7 depicts the levels of cardiac markers in control non-diabetic, diabetic and SCP-D-P nanocomposites treated diabetic induced rats. Diabetic induced untreated rats shown significant increase in the levels of creatine kinase and lactate dehydrogenase compared to the control rats. SCP-D-P nanocomposites treated diabetic induced rats shown decrease in the levels of creatine kinase and lactate dehydrogenase compared to the diabetic induced rats. Lipid peroxidation and nitric oxide levels were decreased in SCP-D-P nanocomposites treated diabetic induced rats compared to diabetic induced rats. The antioxidants glutathione, catalase, superoxide dismutase and glutathione-S-transferase were increased in SCP-D-P nanocomposites treated diabetic induced rats compared to the diabetic induced rats.

3.3. Anti-inflammatory effect of SCP-D-P nanocomposites in diabetic induced rats

Fig. 8 illustrates the levels of pro inflammatory markers TNF- α and IL-1 β in control and SCP-D-P nanocomposites treated diabetic induced rats. Both the inflammatory cytokines were increased in diabetic induced rats compared to control rats whereas SCP-D-P nanocomposites treated diabetic induced rats shown significant decrease in the level proinflammatory cytokines compared diabetic induced untreated rats.

3.4. Effect of SCP-D-P nanocomposites of cardiac tissues of diabetic induced rats

The longitudinal section of H&E stained cardiac tissues of non diabetic and SCP-D-P nanocomposites treated diabetic induced rats were photographed and the representative images were depicted in Fig. 9. Fig. 9A shows normal cardiac fibers without any shrinkage or congestion of interfibillar capillaries. Diabetic induced rats shown increased shrinkage of cardiac fibers and interfibillar capillaries congestion (Fig. 9B). SCP-D-P nanocomposites treatment decreased the diabetes induced damage both the low dose and high shown normal cardiac fiber tissue. Compared high dose SCP-D-P nanocomposites treated rats (Fig. 9D) low dose SCP-D-P nanocomposites treated rats shown slight shrinkage of cardiac fibers (Fig. 9C).

3.5. Effect of SCP-D-P nanocomposites on p62/Keap1/Nrf2 signaling in diabetic induced rats

p62/Keap1/Nrf2 signaling plays a vital role in preventing myocardial ischemia hence we assessed the effect of SCP-D-P nanocomposites in diabetic induced rats. Diabetic induction decreased the gene expression of key signaling molecules p62, Keap1, Nrf2 in the cardiac tissue. SCP-D-P nanocomposites treatment significantly increased the gene expression of p62, Keap1, Nrf2 in cardiac tissue of diabetic induced rats thereby prevented the diabetic induced cardiac damage (Fig. 10).

4. Discussion

Nanobiotechnology is a blooming field which had spread its wings in almost all the areas of diagnosis, drug delivery system, nanomedicine etc. Nanocomposites are materials which possess unique properties such as enhanced chemical reactivity, biocompatibility, increased surface area, biodegradability and non toxic in nature. They are highly dispersible in aqueous medium (Kaurav et al., 2018). Nanocomposites were synthesized with various natural polymers such as polyethylene glycol, starch, chitosan etc. Chitosan is a polysaccharide which is non toxic, biocompatible and interacts with biomolecules (Manek et al., 2020; Hu et al., 2011). Polyethylene glycol are highly soluble in water and non toxic, they possess antibacterial property (Kalarikkal et al., 2020). Hence in the current study we synthesized nanocomposites with chitosan-polyethylene glycol. Various metallic and metal oxide nanoparticles were utilized in nanocomposite synthesis zinc oxide, gold, Iron (III) oxide, tin oxide etc. In the present study we used tin oxide nanoparticles which possess numerous pharmacological properties.

Phytochemicals such as terpenoids, flavanoids, polyphenols, tannins, steroids are used to various ailments and they are effective and don't render any side effects. D-Pinitol is one such phytochemical widely distributed as inositol ether in plants belonging to the family of Leguminosae (Christou et al., 2019; González-Mauraza et al., 2016). D-Pinitol possess numerous medicinal properties such

as anti-inflammatory, antidiabetic, antioxidant, antitumour, antibacterial etc (Sánchez-Hidalgo et al., 2020). The efficacy of D-pinitol on myocardial complications was not yet studied hence in the current study we synthesized tin oxide-chitosan-polyethylene glycol nanocomposite encapsulated with D-pinitol.

The spectroscopic analysis with UV-Vis spectroscopy and photoluminescence spectroscopy confirms the synthesis of tin oxide-chitosan-polyethylene glycol-D-pinitol nanocomposites. SCP-D-P nanocomposites shown ideal XRD pattern indicating the crystalline structure of composite. The functional groups present in the SCP-D-P nanocomposites was analyzed with FTIR analysis. The bands indicating the stretches of tin oxide such as O-H, C=O, C-OH, C=O were observed. The results of Dynamic Light scattering analysis indicates the nanocomposites size as 150 nm which is ideal for a nanodrug. The surface morphology of the nanocomposite was studied with FE-SEM analysis which shown agglomerated spherical structures and the EDAX analysis confirms the presence of tin in nanocomposite. The physical characterization analysis of SCP-D-P nanocomposites confirms the synthesis of a ideal nanocomposite to be utilized in nanomedicine.

Hyperglycemia in diabetic patients leads to various complication, the uncontrolled glucose levels impair organ and tissues. Neuronal and endothelial cells are most susceptible to the hyperglycemic condition hence the diabetic patients with uncontrolled glucose levels are more prone to neuronal diseases (Galicia-Garcia et al., 2020; Merovci et al., 2021). Reports suggest prolonged intake of insulin may increase the risk of hypoglycemic condition in patients which leads to morbidity and mortality (Finfer et al., 2009; McDonnell and Umpierrez, 2012; Hulkower et al., 2014). Thus, maintaining glucose levels in diabetic patients is a critically task, therefore in the present study we assessed the efficacy of SCP-D-P nanocomposites in controlling the glucose. Our results prove SCP-D-P nanocomposites effectively fast and prandial sugar levels. It also increased the insulin levels and c-peptide levels. Previous reports suggests D-pinitol activates PI3K/Akt pathway thereby prevents insulin resistance [18], it also stimulates mobility of glucose transporters (GLUT4) thereby increase the insulin sensitivity (Dang et al., 2010). The reduction in the glucose levels in diabetic induced SCP-D-P nanocomposites treated rats may be due to hypoglycemic effect of D-pinitol.

Diabetes leads to various other complications such as retinopathy, neuropathy, cardiovascular diseases etc. The incidence of cardiovascular diseases is increasing in diabetic patients and the treating such patients are also complicated. The angiographic studies of diabetic patients reveals they are more prone to atherosclerotic diseases (Martín-Timón et al., 2014). Compared to non diabetic patients with myocardial infraction the survival rate is lower in nondiabetic patients (Leon and Maddox, 2015). Ischemic heart disease accounts about 12% of total death incidence and it more common between the age group 34 and 75 yrs (Perugini et al., 2010). The drug which controls glucose levels as well as prevent diabetic induced myocardial diseases is need of today. Therefore we assessed the cardioprotective effect of SCP-D-P nanocomposites in streptozotocin induced diabetic rats.

SCP-D-P nanocomposites decreased the total cholesterol levels in diabetic induced rats and it increased the body weight of rats. Oxidative stress plays a critical role in diabetic induced complications especially in myocardial ischemia. Hyperglycemia leads to increased oxidative stress markers such as TBARS, MDA, oxidative nitrotyrosine, oxidative carbonyl in myocardial ischemia patients and it also lowers the antioxidant levels (Rösen et al., 2001). Cell culture study with aortic smooth muscle cells confirms the ROS production during diabetic condition. In the present study also diabetic rats showed decreased levels of antioxidants and increased level of reactive oxygen species. SCP-D-P nanocomposites treatment significantly decreased the oxidative stress levels and

increased the levels of antioxidants (Inoguchi et al., 2000). Choi et al. (2009) demonstrated D-pinitol decreased lipid peroxidation, reduces liver enzymes induces hypercholesterolemia. D-Pinitol increased the antioxidant enzymes in diabetic induced and decreased the reactive oxygen species. Our study correlates with, the increase in antioxidant status by SCP-D-P nanocomposites treatment may be due to the antioxidant property of D-pinitol.

Echocardiography analysis of Type1 diabetic patients shown early diastolic and atrial filling, increased supra ventricular premature bears causing diastolic dysfunction. Patients with asymptomatic diabetes are more prone to left ventricular diastolic dysfunction causing stiffness of myocardial and vascular tissues (Kenchaiah and Vasan, 2015). Our echocardiography results have proven SCP-D-P nanocomposites have decreased the left ventricular end systolic and diastolic diameter, increased the left ventricular ejection fraction in diabetic induced rats. It also decreased the myocardial ischemia marker protein N-terminal proatriuretic peptide this correlates which indicates SCP-D-P nanocomposites decreases the risk myocardial ischemia in diabetic rats. Inflammation, is a key player of initiation, progression and complication of myocardial ischemia, hence in the current study we assessed the anti-inflammatory property of SCP-D-P nanocomposites in diabetic induced rats. SCP-D-P nanocomposites significantly decreased the levels of proinflammatory cytokines TNF- α and IL-1 β protein there by prevented diabetic induced inflammation. Further our histopathological analysis of cardiac tissue confirms SCP-D-P nanocomposites prevented myocardial ischemia in diabetic induced rats.

NRF2/KEAP1 pathway is signaling pathway involved in generation of antioxidant enzymes to protect cells from oxidative stress. During normal state NRF2 binds with KEAP1 and remains cytoplasm, during stress conditions NRF2 disassociates from KEAP1 and translocates to the nucleus to activate antioxidant response element (ARE) leading to the synthesis of downstream signaling proteins (Tan et al., 2020). p62 a selective autophagy adaptor protein, aggregation of p62 protein with NRF2/KEAP1 enhances the disassociation of NRF2/KEAP1 binding thereby promotes NRF2 nuclear translocation. Thus activating the NRF2/KEAP1/p62 signaling pathway in diabetic induced myocardial ischemic patients will decrease the oxidative stress and increase antioxidant enzymes. In our study SCP-D-P nanocomposites significantly increased the gene expression of NRF2, KEAP1 and p62 signaling proteins thereby prevented diabetic induced oxidative stress which leads to myocardial ischemia.

5. Conclusion

To conclude, in our present study we synthesized tin oxide-Chitosan-Polyethylene glycol nanocomposite with D-Pinitol and assessed the efficacy of SCP-D-P nanocomposites on ameliorating cardiac ischemia in diabetic induced rats. Our characterization analysis of SCP-D-P nanocomposites has proven it has a potent nanodrug. SCP-D-P nanocomposites treatment have effectively decreased the levels of glucose and increased the levels of antioxidants in diabetic induced rats. Echocardiography analysis have proven SCP-D-P nanocomposites treatment have prevented the rats from diabetic induced myocardial ischemia, it was further confirmed with our histopathological analysis of cardiac tissue SCP-D-P nanocomposites treated diabetic induced rats. SCP-D-P nanocomposites activated NRF2/KEAP1/p62 signaling proteins this may be the reason for increase in antioxidants which would have prevented SCP-D-P nanocomposites treated rats from diabetic induced myocardial ischemia. Overall, our results proves SCP-D-P nanocomposites is a potent drug for diabetic patients to prevent

myocardial ischemia with further clinical trials it can authentically proved.

Funding

National Natural Science Foundation of China (NSFC. 82000786) and the Key Research and Development Program of Shaanxi Province (2020SF-248).

Declaration of Competing Interest

The authors declare that they have no known competing financial interests or personal relationships that could have appeared to influence the work reported in this paper.

References

- Ali, A., Ahmed, S., 2018. A review on chitosan and its nanocomposites in drug delivery. *Int. J. Biol. Macromol.* 109, 273–286.
- Arnold, S.V., Bhatt, D.L., Barsness, G.W., Beatty, A.L., Deedwania, P.C., Inzucchi, S.E., Kosiborod, M., Leiter, L.A., Lipska, K.J., Newman, J.D., Welty, F.K., American Heart Association Council on Lifestyle and Cardiometabolic Health and Council on Clinical Cardiology, 2020. Clinical management of stable coronary artery disease in patients with type 2 diabetes mellitus: A scientific statement from the American Heart Association. *Circulation* 141 (19), e779–e806.
- Bommer, C., Heesemann, E., Sagalova, V., Manne-Goehler, J., Atun, R., Bärnighausen, T., Vollmer, S., 2017. The global economic burden of diabetes in adults aged 20–79 years: a cost-of-illness study. *Lancet Diabetes Endocrinol.* 5 (6), 423–430.
- Chadha, S., 2013. Nanotechnology and its application. *IAFST*, 1011–1018.
- Cho, N.H., Shaw, J.E., Karuranga, S., Huang, Y., da Rocha Fernandes, J.D., Ohlrogge, A.W., Malanda, B., 2018. IDF Diabetes Atlas: Global estimates of diabetes prevalence for 2017 and projections for 2045. *Diabetes Res. Clin. Pract.* 138, 271–281.
- Choi, M.-S., Lee, M.-K., Jung, U.J., Kim, H.-J., Do, G.-M., Park, Y.B., Jeon, S.-M., 2009. Metabolic response of soy pinitol on lipid-lowering, antioxidant and hepatoprotective action in hamsters fed-high fat and high cholesterol diet. *Mol. Nutr. Food Res.* 53 (6), 751–759.
- Christou, C., Poulli, E., Yiannopoulos, S., Agapiou, A., 2019. GC-MS analysis of D-pinitol in carob: Syrup and fruit (flesh and seed). *J. Chromatogr. B Analyt. Technol. Biomed. Life Sci.* 1116, 60–64.
- Dang, N.T., Mukai, R., Yoshida, K., Ashida, H., 2010. D-pinitol and myo-inositol stimulate translocation of glucose transporter 4 in skeletal muscle of C57BL/6 mice. *Biosci. Biotechnol. Biochem.* 74 (5), 1062–1067.
- Dedov, I.I., Shestakova, M.V., Vikulova, O.K., 2015. National register of diabetes mellitus in Russian Federation. *Diabetes Mell.* 18 (3), 5–22.
- Ferannini, G., Manca, M.L., Magnoni, M., Andreotti, F., Andreini, D., Latini, R., Maseri, A., Maggioni, A.P., Ostroff, R.M., Williams, S.A., Ferrannini, E., 2020. Coronary artery disease and type 2 diabetes: a proteomic study. *Diabetes Care* 43 (4), 843–851.
- Finfer, S., Chittock, D.R., Su, S.Y., Blair, D., Foster, D., Dhingra, V., Bellomo, R., Cook, D., Dodek, P., Henderson, W.R., Hébert, P.C., Heritier, S., Heyland, D.K., McArthur, C., McDonald, E., Mitchell, I., Myburgh, J.A., Norton, R., Potter, J., Robinson, B.G., Ronco, J.J., 2009. Intensive versus conventional glucose control in critically ill patients. *N. Engl. J. Med.* 360 (13), 1283–1297.
- Galicia-García, U., Benito-Vicente, A., Jebari, S., Larrea-Sebal, A., Siddiqi, H., Uribe, K. B., Ostolaza, H., Martín, C., 2020. Pathophysiology of type 2 diabetes mellitus. *Int. J. Mol. Sci.* 21 (17), 6275.
- Gao, Y., Zhang, M., Wu, T., 2015. Effects of D-pinitol on insulin resistance through the PI3K/Akt signaling pathway in type 2 diabetes mellitus rats. *J. Agric. Food Chem.* 63, 6019–6026.
- GBD 2013 Mortality and Causes of Death Collaborators. Global, regional, and national age-sex specific all-cause and cause-specific mortality for 240 causes of death, 1990–2013: a systematic analysis for the Global Burden of Disease Study 2013. *Lancet.* 2015;385(9963):117–71.
- González-Mauraza, N.H., León-González, A.J., Espartero, J.L., Gallego-Fernández, J.B., Sánchez-Hidalgo, M., Martín-Cordero, C., 2016. Isolation and quantification of pinitol, a bioactive cyclitol, in *Retama* spp. *Nat. Prod. Commun.* 11, 405–406.
- Harding, J.L., Pavkov, M.E., Magliano, D.J., Shaw, J.E., Gregg, E.W., 2019. Global trends in diabetes complications: a review of current evidence. *Diabetologia* 62 (1), 3–16.
- Hu, Y.L., Qi, W., Han, F., Shao, J.Z., Gao, J.Q., 2011. Toxicity evaluation of biodegradable chitosan nanoparticles using a zebrafish embryo model. *Int. J. Nanomed.* 6, 3351–3359.
- Hulkower, R.D., Pollack, R.M., Zonszein, J., 2014. Understanding hypoglycemia in hospitalized patients. *Diab. Manag. (Lond)* 4 (2), 165–176.
- Inoguchi, T., Li, P., Umeda, F., Yu, H.Y., Kakimoto, M., Imamura, M., Aoki, T., Etoh, T., Hashimoto, T., Naruse, M., Sano, H., Utsumi, H., Nawata, H., 2000. High glucose level and free fatty acid stimulate reactive oxygen species production through protein kinase C-dependent activation of NAD(P)H oxidase in cultured vascular cells. *Diabetes* 49 (11), 1939–1945.
- Kalarikkal, S.P., Prasad, D., Kasiappan, R., Chaudhari, S.R., Sundaram, G.M., 2020. A cost-effective polyethylene glycol-based method for the isolation of functional edible nanoparticles from ginger rhizomes. *Sci. Rep.* 10 (1), 4456.
- Kaurav, H., Manchanda, S., Dua, K., Kapoor, D.N., 2018. Nanocomposites in controlled & targeted drug delivery systems. *NHC* 20, 27–45.
- Kenchaiah, S., Vasan, R.S., 2015. Heart failure in women—insights from the Framingham Heart Study. *Cardiovasc. Drugs Ther.* 29 (4), 377–390.
- Lahuta, L.B., Szablińska, J., Ciak, M., Górecki, R.J., 2018. The occurrence and accumulation of D-pinitol in fenugreek (*Trigonella foenum graecum* L.). *Acta Physiol. Plant.* 40, 155–166.
- Lee, B.H., Lee, C.C., Wu, S.C., 2014. Ice plant (*Mesembryanthemum crystallinum*) improves hyperglycaemia and memory impairments in a Wistar rat model of streptozotocin-induced diabetes. *J. Sci. Food Agric.* 94 (11), 2266–2273.
- Lee, E., Lim, Y., Kwon, S.W., Kwon, O., 2019. Pinitol consumption improves liver health status by reducing oxidative stress and fatty acid accumulation in subjects with non-alcoholic fatty liver disease: A randomized, double-blind, placebo-controlled trial. *J. Nutr. Biochem.* 68, 33–41.
- Leon, B.M., Maddox, T.M., 2015. Diabetes and cardiovascular disease: Epidemiology, biological mechanisms, treatment recommendations and future research. *World J. Diab.* 6 (13), 1246–1258.
- Lin, T.H., Tan, T.-W., Tsai, T.-H., Chen, C.-C., Hsieh, T.-F., Lee, S.-S., Liu, H.-H., Chen, W.-C., Tang, C.-H., 2013. D-pinitol inhibits prostate cancer metastasis through inhibition of $\alpha v \beta 3$ integrin by modulating FAK, c-Src and NF- κ B pathways. *Int. J. Mol. Sci.* 14 (5), 9790–9802.
- Manek, E., Darvas, F., Petroianu, G.A., 2020. Use of biodegradable, chitosan-based nanoparticles in the treatment of Alzheimer's disease. *Molecules* 25 (20), 4866.
- Martín-Timón, I., Sevillano-Collantes, C., Segura-Galindo, A., Del Cañizo-Gómez, F.J., 2014. Type 2 diabetes and cardiovascular disease: Have all risk factors the same strength? *World J. Diab.* 5 (4), 444–470.
- McDonnell, M.E., Umpierrez, G.E., 2012. Insulin therapy for the management of hyperglycemia in hospitalized patients. *Endocrinol. Metab. Clin. North Am.* 41 (1), 175–201.
- Merovci, A., Tripathy, D., Chen, X., Valdez, I., Abdul-Ghani, M., Solis-Herrera, C., Gastaldelli, A., De Fronzo, R.A., 2021. Effect of mild physiologic hyperglycemia on insulin secretion, insulin clearance, and insulin sensitivity in healthy glucose-tolerant subjects. *Diabetes* 70 (1), 2014–2213.
- Perugini, E., Maggioni, A.P., Bocconelli, A., Di Pasquale, G., 2010. Epidemiologia delle sindromi coronariche acute in Italia [Epidemiology of acute coronary syndromes in Italy]. *G Ital Cardiol (Rome)*, 11(10):718–29. Italian.
- Rengarajan, T., Nandakumar, N., Balasubramanian, M.P., 2012. D-Pinitol a low-molecular weight cyclitol prevents 7,12-Dimethylbenz[a]anthracene induced experimental breast cancer through regulating anti-apoptotic protein Bcl-2, mitochondrial and carbohydrate key metabolizing enzymes. *Phytochem. Rev. Biomed. Prev. Nutr.* 2 (1), 25–30.
- Roopan, S.M., Kumar, S.H.S., Madhumitha, G., Suthindhiran, K., 2015. Biogenic production of SnO₂ nanoparticles and its cytotoxic effect against hepatocellular carcinoma cell line (HepG2). *Appl. Biochem. Biotechnol.* 175 (3), 1567–1575.
- Rösen, P., Nawroth, P.P., King, G., Moller, W., Tritschler, H.-J., Packer, L., 2001. The role of oxidative stress in the onset and progression of diabetes and its complications: a summary of a Congress Series sponsored by UNESCO-MCBN, the American Diabetes Association and the German Diabetes Society. *Diabetes Metab. Res. Rev.* 17 (3), 189–212.
- Sánchez-Hidalgo, M., León-González, A.J., Gálvez-Peralta, M., González-Mauraza, N. H., Martín-Cordero, C., 2020. D-Pinitol: a cyclitol with versatile biological and pharmacological activities. *Phytochem. Rev.* 20, 211–224.
- Tan, X., Yang, Y., Xu, J., Zhang, P., Deng, R., Mao, Y., He, J., Chen, Y., Zhang, Y., Ding, J., Li, H., Shen, H., Li, X., Dong, W., Chen, G., 2020. Luteolin exerts neuroprotection via modulation of the p62/Keap1/Nrf2 pathway in intracerebral hemorrhage. *Front. Pharmacol.* 10, 1551.
- Vidhu, V.K., Philip, D., 2015. Biogenic synthesis of SnO₂ nanoparticles: evaluation of antibacterial and antioxidant activities. *Spectrochim. Acta A Mol. Biomol. Spectrosc.* 134, 372–379.
- World Health Organization (WHO) Expert Committee. *Global Report on Diabetes* (World Health Organization, Geneva, 2016).
- Zheng, K., Zhao, Z., Lin, N., Wu, Y., Xu, Y., Zhang, W., 2017. Protective effect of pinitol against inflammatory mediators of rheumatoid arthritis via inhibition of protein tyrosine phosphatase non-receptor type 22 (PTPN22). *Med. Sci. Monit.* 23, 1923–1932.